Condensation Heat Transfer Analysis for Turbine Steam Extraction Points for SMR–TES Integration

Takhyun Chun [a], Gyudong Kim [a], Yong Jae Chae [a], Jeong Ik Lee [a*]
[a]*Department of Nuclear and Quantum Engineering, Korea Advanced Institute of Science and Technology (KAIST), 291 Daehak-ro, Yuseong-gu, Daejeon 34141, Republic of Korea*
[*]*Corresponding author: jeongiklee@kaist.ac.kr*

Keywords : SMR, TES, Condensation, Two-phase flow

1. Introduction

The International Energy Agency (IEA) reports that CO_2 emissions from electricity generation remain the highest among all sectors [1], underscoring the importance of clean generation technologies that can also provide operational flexibility. Meanwhile, the global push for power-sector decarbonization continues to accelerate, and the increasing penetration of variable renewable energy sources further intensifies the challenge of balancing electricity supply and demand. Solar PV and wind power, in particular, are constrained by relatively low capacity factors, whereas nuclear power plants typically achieve higher capacity factors than intermittent renewables, as shown in Table I, enabling them to deliver a more consistent and reliable supply of electricity.

In this context, pressurized water reactors (PWRs), including small modular reactors (SMRs), are increasingly considered not only as reliable low-carbon generators but also as candidates for controlled output modulation in renewable-dominant grids. SMRs offer a compact and modular architecture with potential benefits in construction schedule risk and siting flexibility as depicted in Fig. 1.

Part-load operation in nuclear plants is commonly implemented through reactor thermal-power control. However, frequent changes in reactor power can impose additional operational and safety burdens. Therefore, an effective load-following strategy should minimize primary-side power variations whenever possible. Motivated by this requirement, the present study investigates SMR power cycle integrated with thermal energy storage (TES) to provide grid-level flexibility while mitigating variations in reactor thermal output.

TES stores energy as heat during periods of reduced grid demand and releases the stored heat to support electricity production during peak demand. Sensible-heat TES using low-cost media (e.g., concrete or volcanic rock) is often considered cost-competitive for large-scale storage compared with electrochemical options. Common TES configurations include two-tank systems (e.g., thermal oil or molten salt), packed-bed systems, and shell-and-tube systems in which a storage medium occupies the shell side. This study focuses on a shell-and-tube charging configuration in which extracted turbine steam flows inside the tubes and transfers heat to the storage medium.

In the proposed configuration, extracted turbine steam enters the TES heat exchanger and delivers heat to the storage medium through internal condensation in pipes. Since the latent heat released during condensation typically dominates the stored energy, efficient condensation heat transfer is a key determinant of TES charging performance.

Accordingly, this work compares two candidate extraction locations—upstream of the high-pressure turbine and upstream of the low-pressure turbine—to identify which extraction point is more favorable for charging from a condensation heat-transfer perspective. For the given TES design parameters, the in-tube condensation flow regime is identified, and corresponding heat-transfer correlations are applied. Based on this framework, the study proposes a guideline for selecting turbine steam extraction points for TES integration in the considered SMR power-cycle layout. The proposed methodology is applicable to TES concepts employing shell-and-tube heat exchangers and supports the design of TES-integrated SMR power systems that enhance grid flexibility while preserving reactor stability and cycle performance.

Table I : Capacity factors of power sources [2]

Power source	Capacity factor	Installed capacity
Solar PV	0.13*	151.34 GW
Wind	0.20*	98.37 GW
Nuclear	0.86*	23.53 GW

* Average capacity factor from 2013 to 2022.

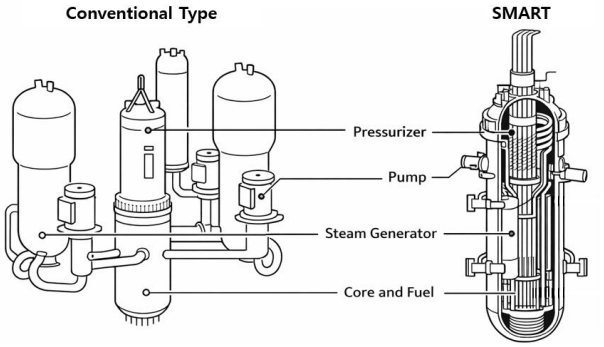

Fig. 1. Comparison of the configurations of conventional PWR (left) and SMART-PWR type SMR (right) [3]

2. SMR power cycle

Fig. 2 provides a schematic of the SMR power conversion system considered in this study. The cycle configuration is partially derived from the NuScale steam-cycle design [4], a representative PWR secondary-side Rankine cycle. The cycle layout is a hypothetical configuration developed in this work, in which major components (e.g., turbines and feedwater heaters) are explicitly modeled to construct the full system.

The steady-state operating conditions, parameters, and performance of the SMR power cycle are listed in Table II. Based on the resulting steady-state cycle, a heat-transfer analysis was conducted at the turbine steam extraction locations using the thermodynamic properties evaluated at the corresponding extraction conditions. Two extraction locations were examined in this study: the inlet of the high-pressure turbine (HPT) and the inlet of the low-pressure turbine (LPT).

Fig. 3 shows the on-design T–s diagram for the SMR power cycle used in this study. The diagram illustrates the major thermodynamic processes, including feedwater heating in the Feed Water Heaters (FWHs), steam generation in the SG, expansion through the turbine stages, and condensation in the condenser. For TES charging, a portion of the steam is extracted to store thermal energy in the TES, and the resulting condensate is routed to the deaerator (DA) as depicted in Figs. 5 and 6. This extraction reduces the steam flow admitted to the turbine, allowing the power cycle net turbine work output to be adjusted to match the load demand.

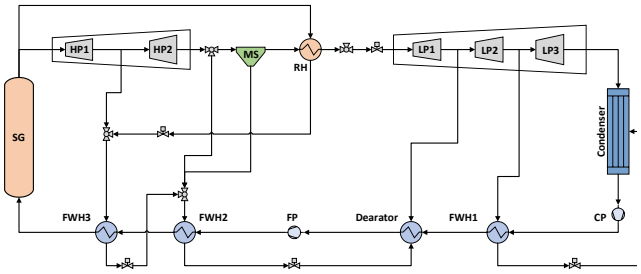

Fig. 2. Layout of SMR used in this study

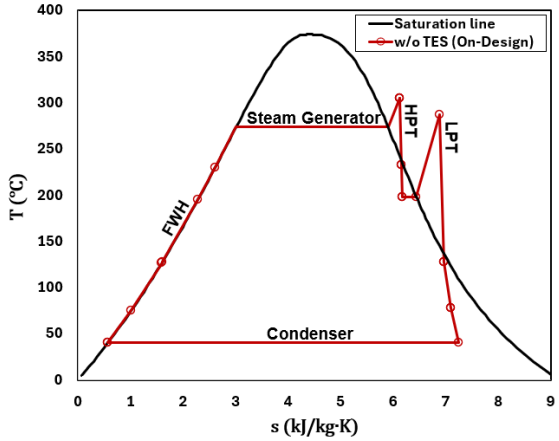

Fig. 3. Steady-state T-s diagram of the SMR power cycle

Table II. Cycle parameters/conditions for on-design

Cycle Conditions	Value
SG thermal power	600 MWth
SG outlet pressure	5.82 MPa
SG outlet temperature	304.8 °C
SG inlet temperature	230.0 °C
Condenser outlet temperature	40 °C
Feedwater mass flow rate	312.8 kg/s
Cycle Parameters	Value
Turbine efficiency	90%
Pump efficiency	80%
Generator efficiency	95%
HPT work	66.9 MW
LPT work	151.7 MW
Pump work	2.56 MW
Net efficiency	34.2 %

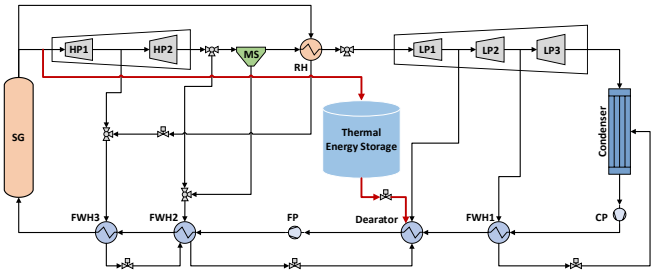

Fig. 4. SMR layout for TES integration from HPT inlet to DA for charging

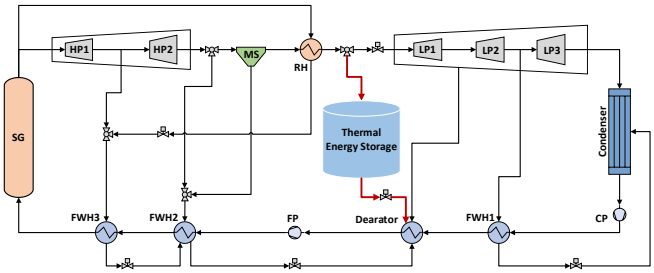

Fig. 5. SMR layout for TES integration from HPT inlet to DA for charging

3. Condensation Heat Transfer Analysis

During TES charging with the shell-and-tube configuration, superheated steam flows through the tubes and transfers heat to the thermal energy storage medium. As heat is removed, the vapor cools toward saturation and subsequently undergoes condensation. In this process, the latent heat released during condensation is typically much larger than the sensible heat associated with cooling the superheated vapor. Because TES charging performance is governed primarily by condensation, the performance trends should be evaluated under two-phase conditions, where condensation effects control the overall heat-transfer behavior. Accordingly, an appropriate condensation heat-transfer correlation must be applied.

In this study, a tube bundle which consists of 1,000 is selected to maintain turbulent flow, with Reynolds numbers exceeding 10,000 at the inlet. The tube outer diameter was fixed at 1 1/2 inch, which is a typical value recommended in standard heat exchanger design guidelines [5,6], in order to examine the overall trend under a representative geometric condition. The selected geometric parameters are summarized in Table III.

The analysis is conducted using the inlet condition corresponding to a mass flow rate of 20 kg/s. The resulting flow condition varies depending on the geometric parameters such as tube inner diameter and number of tubes, and the mass flow rate. Accordingly, the flow regime and the heat transfer coefficient also vary. In the present study, the analysis was therefore limited to representative horizontal plain-tube geometry and extraction flow condition.

To account for condensation behavior, the Breber map is employed to identify the two-phase flow pattern, and a correlation consistent with the identified regime is applied. The flow regime for each case is determined using Eqs. (1) and (2). In Eq. (1), the Martinelli parameter X, defined as the square root of the ratio of liquid to vapor frictional pressure gradients, is approximated in terms of the vapor quality x. In Eq. (2), the dimensionless gas velocity used in the Breber map is a modified form of the Wallis dimensionless gas velocity, representing a Froude-number-related nondimensional parameter. The resulting flow patterns on the Breber map are shown in Fig. 6 [7].

$$X = \sqrt{\frac{\left(\frac{dP}{dz}\right)_f}{\left(\frac{dP}{dz}\right)_g}} \cong \left(\frac{1-x}{x}\right)^{0.875} \left(\frac{\nu_f}{\nu_g}\right)^{0.5} \left(\frac{\mu_f}{\mu_g}\right)^{0.125} \quad (1)$$

$$j^*_{g,Breber} = \frac{G}{\sqrt{D_i \cdot g \cdot \rho_g (\rho_f - \rho_g)}} \cdot \left(\frac{\mathrm{K_p}}{\mathrm{X}^{1.111} + K_p}\right) \quad (2)$$

$$\text{where, } \mathrm{K_p} = \left(\frac{\rho_g}{\rho_f}\right)^{0.555} \left(\frac{\mu_f}{\mu_g}\right)^{0.111}$$

Stratified and wavy flows are not distinguished on the Breber map. However, the heat-transfer regime selection in Shah's condensation framework depends on whether the flow is classified as stratified or stratified–wavy. To remove this ambiguity, the Taitel–Dukler map was additionally constructed, as shown in Fig. 7 [8]. The K_{TD} values from Eq. (3) were found to lie above Boundary C in Fig. 7. Accordingly, the Zone 2 conditions identified from the Breber map (Fig. 6) were classified as stratified–wavy flow.

$$K_{TD} = \left(\frac{\rho_g \, j_g^2 \, j_f}{(\rho_f - \rho_g) \, g \left(\frac{\mu}{\rho}\right)_f \cos\theta}\right)^{1/2} \quad (3)$$

Depending on the flow pattern, Shah suggested using various heat transfer correlations [9]. Based on Shah's work [9, 10], regime-dependent correlations were used in this study, and heat transfer correlations for flow pattern were summarized in Table IV.

Table III. Geometrical parameters TES in this study

Geometrical parameters	Value
Tube outer diameter (OD)	0.0381 m
Tube inner diameter	0.0297 m
Tube thickness	0.00419 m
Number of tubes	1,000

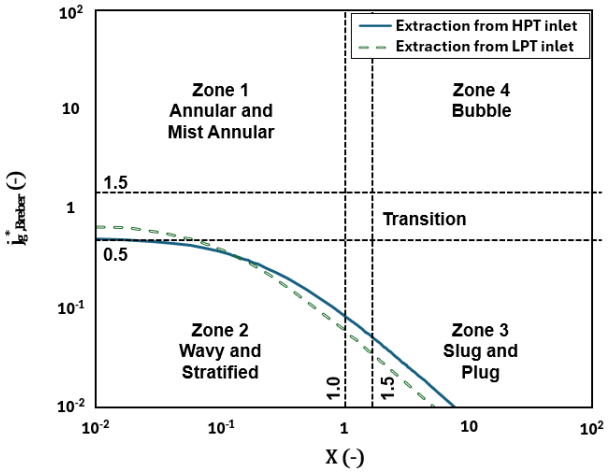

Fig. 6. Identification of flow pattern on the Breber map

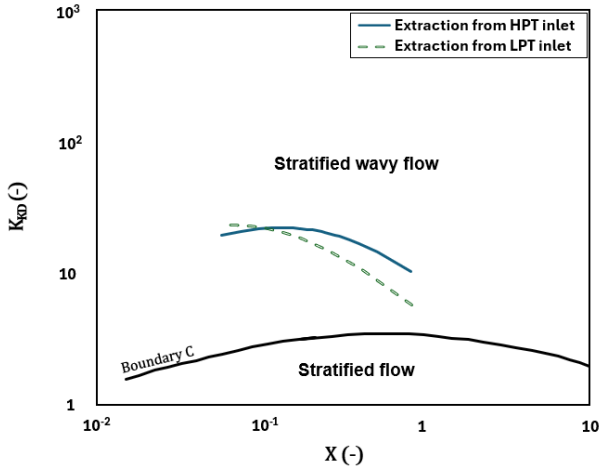

Fig. 7. Identification of stratified and stratified-wavy on the Taitel-Dukler map

Table IV. Heat transfer correlations by Shah's correlations [9, 10]

Flow pattern	Correlations
Annular & Mist annular flow	$h_{TP} = h_l = h_{LS}\left(1 + \frac{3.8}{Z^{0.95}}\right)\left(\frac{\mu_f}{14 \cdot \mu_g}\right)^{0.0058+0.557 \cdot P_r}$ where $h_{LS} = 0.023\, Re_{LS}^{0.8}\, Pr_f^{0.4} k_f / D_i$,

	$Z = \left(\frac{1}{x} - 1\right)^{0.8} P_r^{0.4}\ ,\ P_{re} = P/P_c$
Stratified-wavy flow	$h_{TP} = h_l + h_{Nu}$ $= h_l + 1.32 * Re_{LS}^{-\frac{1}{3}} \left[\frac{\rho_f \left(\rho_f - \rho_g\right) g\, k_f^3}{\mu_f^2}\right]^{1/3}$
Slug & Plug flow (intermittent)	$h_{TP} = h_l$

4. Results and Discussions

The flow during condensation in this study starts from the annular–wavy transition phase, changes into stratified–wavy flow, and then stays in slug or plug flow until condensation is finished. The correlations for the two nearby regimes were linearly interpolated to produce the heat transfer coefficients in the transition zone. Fig. 8 shows the obtained heat transfer coefficients as a function of vapor quality.

The results indicate that, under high-pressure conditions above approximately 10 bar, steam condensation heat transfer is strongly influenced by pressure. For the SMR power-cycle layout and the inner diameter and number of tubes considered in this study, the condensation heat-transfer coefficient at the HPT inlet condition (58 bar) was approximately 10^4 times higher than that at the LPT inlet condition (14 bar) for the same mass flow rate of 20 kg/s. This condensation heat-transfer assessment can serve as a quantitative basis for determining the more suitable steam extraction location between HPT inlet and LPT inlet when integrating TES into an SMR power cycle.

However, since the total thermal resistance will be consisted of condensation heat transfer and conduction heat transfer of the thermal energy storing medium, the major bottleneck for the total thermal resistance will be on the solid conduction side. Therefore, the improvement of the condensation heat transfer may not be substantially influencing the design once the heat transfer coefficient become larger than certain value.

For the representative geometry and flow condition considered in this study, the higher-pressure HPT extraction was predicted to yield a larger tube-side condensation heat transfer coefficient than the LPT extraction as shown in Fig. 8. To generalize this trend further, additional studies covering a wider range of geometric parameters and flow conditions are required.

Additionally, steam extraction to the TES requires the prior availability of a valve capable of operating at the temperature and pressure conditions at the selected extraction point on the main steam line. In actual large-scale nuclear or fossil-fired steam power plants, turbine extraction steam lines are sometimes isolated during startup or shut down by means of turbine isolation valves. However, since industrial practice has not yet established a specific standard for how extraction control should be implemented for TES integration, it is difficult to define a single valve type as the definitive option. Candidate valves for branching flow from the main steam line to the TES while enabling extraction flow control include three-way diverting valves, two-port globe control valves, and two-port angle-body control valves.

For the high-temperature and high-pressure conditions considered in this study, approximately 300°C and up to 60 bar, valves with a pressure rating of at least Class 600 are generally required [11]. If only the extraction condition upstream of the LPT is considered, ASME Class 300 rating may also be feasible. The final valve selection should be determined through further detailed design, considering additional considerations such as valve capacity, allowable pressure drop, noise [12].

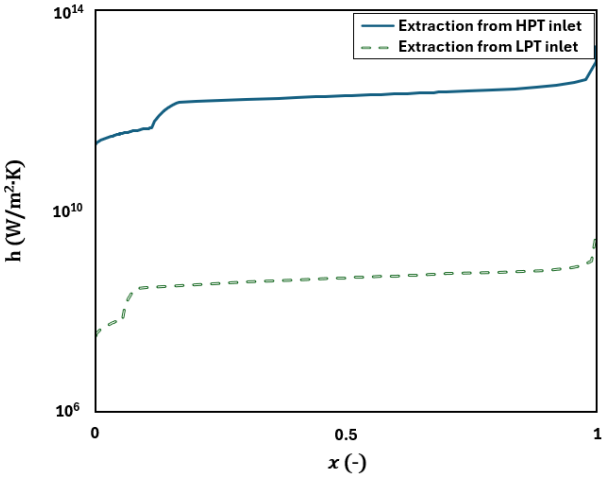

Fig. 8. Predicted heat transfer coefficient as a function of vapor quality using Shah's correlations

5. Summary and Conclusions

This study investigates the integration of a thermal energy storage (TES) system with a PWR-type SMR power cycle to enable load-following operation. Motivated by the increasing demand for grid flexibility under rising renewable penetration, the study provides a guideline for selecting turbine steam extraction locations based on steam condensation heat transfer, which governs TES charging performance. The proposed TES is assumed to be a shell-and-tube, where extracted turbine steam flows through the tubes, is cooled and condensed, and transfers heat to the storage medium during charging.

Since condensation heat transfer in the charging section varies strongly with the two-phase flow pattern, the present work first identifies the flow regime using the Breber map and then applies the Taitel–Dukler map to reduce ambiguity within stratified flow regions by distinguishing stratified–wavy flow. Flow pattern dependent condensation correlations following Shah are subsequently employed to predict the condensation heat-transfer coefficient as a function of vapor quality x. The analysis considers a tube bundle of 1,000 tubes with an inner diameter of 0.0297 m at an extraction mass flow rate of 20 kg/s. Under the considered cycle, geometry, and flow conditions, pressure effects significantly

intensify condensation heat transfer, and the condensation heat-transfer coefficient at the HPT inlet is predicted to be on the order of 10^4times larger than that at the LPT inlet.

However, selecting the extraction location solely based on condensation heat transfer is insufficient because the TES charging rate is governed by the total thermal resistance of the entire system. In particular, from an overall thermal-resistance perspective, conduction through the storage medium can dominate over the tube-side condensation resistance, potentially limiting the practical impact of improved condensation heat transfer. Therefore, a coupled assessment that quantifies how the condensation heat-transfer enhancement translates to overall heat-transfer performance is required. For future work, the present analysis will be extended beyond the specific geometric parameters considered in this study to establish more generalizable trends in condensation heat transfer. In addition, to enable a quantitative and reasonable comparison between the HPT inlet and LPT inlet extraction options, further engineering considerations such as exergy and economic analysis associated with differences of thermodynamic states will be incorporated. Ultimately, these extensions are expected to provide a framework for identifying the most suitable steam extraction location for TES integration within the given SMR power-cycle layout.

ACKNOWLEDGEMENTS

This work was supported by the Small Modular Reactor Technology Development Program funded by the Korea government (MOTIE)(No. RS-2024-00400615).

REFERENCES

[1] IEA, *Electricity 2025*, International Energy Agency, Paris, 2025.
[2] Semin Joo, Seok Ho Song, Staffan Qvist, Jeong Ik Lee, “Evaluation of Coal Repowering Option with Small Modular Reactor in South Korea”, Energies., 17, 2024.
[3] Giorgio Locatelli, “Small modular reactors: A comprehensive overview of their economics and strategic aspects”, Progress in Nuclear Energy, Vol 73. 2014. 75-85p
[4] U.S. NRC, *Westinghouse Technology Systems Manual, Section 1.2: Introduction to Pressurized Water Reactor Generating Systems*, Nuclear Regulatory Commission, U.S., 2007.
[5] Byrne, R. C. Tubular Exchanger Manufacturers Association: Standards and Practices. Tubular Exchanger Manufacturers Association, TEMA, 2007.
[6] Kuppan, T. Heat Exchanger Design Handbook. New York: Marcel Dekker, 2000.
[7] Breber, G., Palen, J. W., and Taborek, J., “Prediction of Horizontal Tubeside Condensation of Pure Components Using Flow Regime Criteria,” ASME Journal of Heat Transfer, 102, pp. 471–476, 1980.
[8] Taitel, Y., and Dukler, A. E., “A Model for Predicting Flow Regime Transitions in Horizontal and Near-Horizontal Gas-Liquid Flow,” AIChE Journal, 22, pp. 47–55, 1976.
[9] Shah, M. M. “A New Flow Pattern Based General Correlation for Heat Transfer During Condensation in Horizontal Tubes.” Proceedings of the 15th International Heat Transfer Conference (IHTC-15), Kyoto, Japan, 2014.
[10] Shah, M. M. “An Improved and Extended General Correlation for Heat Transfer During Condensation in Plain Tubes.” HVAC&R Research, pp. 889–913, 2009.
[11] ASME, *Valves—Flanged, Threaded, and Welding*, The American Society of Mechanical Engineers, New York, 2025.
[12] Fisher Controls International LLC, *Control Valve Sourcebook: Oil & Gas*, 2013.